

Measurement of the x - and Q^2 -Dependence of the Asymmetry A_1 on the Nucleon

K.V. Dharmawardane,^{29,*} S.E. Kuhn,^{29,†} P. Bosted,³⁶ Y. Prok,^{39,36,‡} G. Adams,³¹ P. Ambrozewicz,¹¹
M. Anghinolfi,¹⁷ G. Asryan,⁴¹ H. Avakian,^{16,36} H. Bagdasaryan,^{41,29} N. Baillie,⁴⁰ J.P. Ball,² N.A. Baltzell,³⁵
S. Barrow,¹² V. Batourine,²² M. Battaglieri,¹⁷ K. Beard,²¹ I. Bedlinskiy,²⁰ M. Bektasoglu,^{29,§} M. Bellis,^{31,5}
N. Benmouna,¹³ A.S. Biselli,^{31,5} B.E. Bonner,³² S. Bouchigny,^{36,18} S. Boiarinov,^{20,36} R. Bradford,⁵ D. Branford,¹⁰
W.K. Brooks,³⁶ S. Bültmann,²⁹ V.D. Burkert,³⁶ C. Butuceanu,⁴⁰ J.R. Calarco,²⁶ S.L. Careccia,²⁹ D.S. Carman,²⁸
B. Carnahan,⁶ A. Cazes,³⁵ S. Chen,¹² P.L. Cole,^{36,15} P. Collins,² P. Coltharp,¹² D. Cords,^{36,¶} P. Corvisiero,¹⁷
D. Crabb,³⁹ H. Crannell,⁶ V. Crede,¹² J.P. Cummings,³¹ R. De Masi,⁷ R. DeVita,¹⁷ E. De Sanctis,¹⁶
P.V. Degtyarenko,³⁶ H. Denizli,³⁰ L. Dennis,¹² A. Deur,³⁶ C. Djalali,³⁵ G.E. Dodge,²⁹ J. Donnelly,¹⁴ D. Doughty,^{8,36}
P. Dragovitsch,¹² M. Dugger,² S. Dytman,³⁰ O.P. Dzyubak,³⁵ H. Egiyan,^{40,36,**} K.S. Egiyan,⁴¹ L. Elouadrhiri,^{8,36}
P. Eugenio,¹² R. Fatemi,³⁹ G. Fedotov,²⁵ R.J. Feuerbach,⁵ T.A. Forest,²⁹ H. Funsten,⁴⁰ M. Garçon,⁷
G. Gavalian,^{26,29} G.P. Gilfoyle,³⁴ K.L. Giovanetti,²¹ F.X. Girod,⁷ J.T. Goetz,³ E. Golovatch,^{17,††} A. Gonenc,¹¹
R.W. Gothe,³⁵ K.A. Griffioen,⁴⁰ M. Guidal,¹⁸ M. Guillo,³⁵ N. Guler,²⁹ L. Guo,³⁶ V. Gyurjyan,³⁶ C. Hadjidakis,¹⁸
K. Hafidi,¹ R.S. Hakobyan,⁶ J. Hardie,^{8,36} D. Heddle,^{8,36} F.W. Hersman,²⁶ K. Hicks,²⁸ I. Hleiqawi,²⁸ M. Holtrop,²⁶
M. Huertas,³⁵ C.E. Hyde-Wright,²⁹ Y. Iieva,¹³ D.G. Ireland,¹⁴ B.S. Ishkhanov,²⁵ E.L. Isupov,²⁵ M.M. Ito,³⁶
D. Jenkins,³⁸ H.S. Jo,¹⁸ K. Joo,⁹ H.G. Juengst,²⁹ C. Keith,³⁶ J.D. Kellie,¹⁴ M. Khandaker,²⁷ K.Y. Kim,³⁰ K. Kim,²²
W. Kim,²² A. Klein,^{29,‡‡} F.J. Klein,^{11,6} M. Klusman,³¹ M. Kossov,²⁰ L.H. Kramer,^{11,36} V. Kubarovskiy,³¹
J. Kuhn,^{31,5} S.V. Kuleshov,²⁰ J. Lachniet,^{5,29} J.M. Laget,^{7,36} J. Langheinrich,³⁵ D. Lawrence,²⁴ Ji Li,³¹
A.C.S. Lima,¹³ K. Livingston,¹⁴ H. Lu,³⁵ K. Lukashin,⁶ M. MacCormick,¹⁸ J.J. Manak,³⁶ N. Markov,⁹ S. McAleer,¹²
B. McKinnon,¹⁴ J.W.C. McNabb,⁵ B.A. Mecking,³⁶ M.D. Mestayer,³⁶ C.A. Meyer,⁵ T. Mibe,²⁸ K. Mikhailov,²⁰
R. Minehart,³⁹ M. Mirazita,¹⁶ R. Miskimen,²⁴ V. Mokeev,²⁵ L. Morand,⁷ S.A. Morrow,^{18,7} M. Moteabbed,¹¹
J. Mueller,³⁰ G.S. Mutchler,³² P. Nadel-Turonski,¹³ J. Napolitano,³¹ R. Nasseripour,^{11,35} S. Niccolai,^{13,18}
G. Niculescu,^{28,21} I. Niculescu,^{13,21} B.B. Niczyporuk,³⁶ M.R. Niroula,²⁹ R.A. Niyazov,^{29,36} M. Nozar,³⁶
G.V. O'Rielly,¹³ M. Osipenko,^{17,25} A.I. Ostrovidov,¹² K. Park,²² E. Pasyuk,² C. Paterson,¹⁴ S.A. Philips,¹³
J. Pierce,³⁹ N. Pivnyuk,²⁰ D. Pocanic,³⁹ O. Pogorelko,²⁰ E. Polli,¹⁶ S. Pozdniakov,²⁰ B.M. Preedon,³⁵ J.W. Price,⁴
D. Protopopescu,^{26,14} L.M. Qin,²⁹ B.A. Raue,^{11,36} G. Riccardi,¹² G. Ricco,¹⁷ M. Ripani,¹⁷ B.G. Ritchie,²
F. Ronchetti,¹⁶ G. Rosner,¹⁴ P. Rossi,¹⁶ D. Rowntree,²³ P.D. Rubin,³⁴ F. Sabatié,^{29,7} C. Salgado,²⁷
J.P. Santoro,^{38,36,§§} V. Sapunenko,^{17,36} R.A. Schumacher,⁵ V.S. Serov,²⁰ Y.G. Sharabian,³⁶ J. Shaw,²⁴
N.V. Shvedunov,²⁵ A.V. Skabelin,²³ E.S. Smith,³⁶ L.C. Smith,³⁹ D.I. Sober,⁶ A. Stavinsky,²⁰ S.S. Stepanyan,²²
S. Stepanyan,^{36,8,41} B.E. Stokes,¹² P. Stoler,³¹ I.I. Strakovskiy,¹³ S. Strauch,³⁵ R. Suleiman,²³ M. Taiuti,¹⁷
S. Taylor,³² D.J. Tedeschi,³⁵ U. Thoma,^{36,¶¶} R. Thompson,³⁰ A. Tkabladze,¹³ S. Tkachenko,²⁹ L. Todor,⁵
C. Tur,³⁵ M. Ungaro,⁹ M.F. Vineyard,^{37,34} A.V. Vlassov,²⁰ L.B. Weinstein,²⁹ D.P. Weygand,³⁶ M. Williams,⁵
E. Wolin,³⁶ M.H. Wood,^{35,***} A. Yegneswaran,³⁶ J. Yun,²⁹ L. Zana,²⁶ J. Zhang,²⁹ B. Zhao,⁹ and Z. Zhao³⁵

(The CLAS Collaboration)

¹Argonne National Laboratory, Argonne, Illinois 60439

²Arizona State University, Tempe, Arizona 85287-1504

³University of California at Los Angeles, Los Angeles, California 90095-1547

⁴California State University, Dominguez Hills, Carson, CA 90747

⁵Carnegie Mellon University, Pittsburgh, Pennsylvania 15213

⁶Catholic University of America, Washington, D.C. 20064

⁷CEA-Saclay, Service de Physique Nucléaire, F91191 Gif-sur-Yvette, France

⁸Christopher Newport University, Newport News, Virginia 23606

⁹University of Connecticut, Storrs, Connecticut 06269

¹⁰Edinburgh University, Edinburgh EH9 3JZ, United Kingdom

¹¹Florida International University, Miami, Florida 33199

¹²Florida State University, Tallahassee, Florida 32306

¹³The George Washington University, Washington, DC 20052

¹⁴University of Glasgow, Glasgow G12 8QQ, United Kingdom

¹⁵Idaho State University, Pocatello, Idaho 83209

¹⁶INFN, Laboratori Nazionali di Frascati, 00044 Frascati, Italy

¹⁷INFN, Sezione di Genova, 16146 Genova, Italy

¹⁸Institut de Physique Nucleaire ORSAY, Orsay, France

¹⁹Institute für Strahlen und Kernphysik, Universität Bonn, Germany

²⁰Institute of Theoretical and Experimental Physics, Moscow, 117259, Russia

- ²¹James Madison University, Harrisonburg, Virginia 22807
²²Kyungpook National University, Daegu 702-701, South Korea
²³Massachusetts Institute of Technology, Cambridge, Massachusetts 02139-4307
²⁴University of Massachusetts, Amherst, Massachusetts 01003
²⁵Moscow State University, General Nuclear Physics Institute, 119899 Moscow, Russia
²⁶University of New Hampshire, Durham, New Hampshire 03824-3568
²⁷Norfolk State University, Norfolk, Virginia 23504
²⁸Ohio University, Athens, Ohio 45701
²⁹Old Dominion University, Norfolk, Virginia 23529
³⁰University of Pittsburgh, Pittsburgh, Pennsylvania 15260
³¹Rensselaer Polytechnic Institute, Troy, New York 12180-3590
³²Rice University, Houston, Texas 77005-1892
³³Sakarya University, Sakarya, Turkey
³⁴University of Richmond, Richmond, Virginia 23173
³⁵University of South Carolina, Columbia, South Carolina 29208
³⁶Thomas Jefferson National Accelerator Facility, Newport News, Virginia 23606
³⁷Union College, Schenectady, NY 12308
³⁸Virginia Polytechnic Institute and State University, Blacksburg, Virginia 24061-0435
³⁹University of Virginia, Charlottesville, Virginia 22901
⁴⁰College of William and Mary, Williamsburg, Virginia 23187-8795
⁴¹Yerevan Physics Institute, 375036 Yerevan, Armenia
- (Dated: May 6, 2006)

We report results for the virtual photon asymmetry A_1 on the nucleon from new Jefferson Lab measurements. The experiment, which used the CEBAF Large Acceptance Spectrometer and longitudinally polarized proton ($^{15}\text{NH}_3$) and deuteron ($^{15}\text{ND}_3$) targets, collected data with a longitudinally polarized electron beam at energies between 1.6 GeV and 5.7 GeV. In the present paper, we concentrate on our results for $A_1(x, Q^2)$ and the related ratio $g_1/F_1(x, Q^2)$ in the resonance and the deep inelastic regions for our lowest and highest beam energies, covering a range in momentum transfer Q^2 from 0.05 to 5.0 (GeV/c) 2 and in final-state invariant mass W up to about 3 GeV. Our data show detailed structure in the resonance region, which leads to a strong Q^2 -dependence of $A_1(x, Q^2)$ for W below 2 GeV. At higher W , a smooth approach to the scaling limit, established by earlier experiments, can be seen, but $A_1(x, Q^2)$ is not strictly Q^2 -independent. We add significantly to the world data set at high x , up to $x = 0.6$. Our data exceed the SU(6)-symmetric quark model expectation for both the proton and the deuteron while being consistent with a negative d -quark polarization up to our highest x . This data set should improve next-to-leading order (NLO) pQCD fits of the parton polarization distributions.

PACS numbers: 13.60.Hb, 13.88.+e, 14.20.Dh

Keywords: Spin structure functions, nucleon structure

The spin structure of the nucleon has been investigated in a series of much-discussed polarized lepton scattering experiments over the last 25 years [1–13]. These measurements, most of which covered the deep inelastic scattering (DIS) region of large final-state invariant mass W and momentum transfer Q^2 , compared the Q^2 -dependence of the polarized structure function g_1 with QCD expectations and shed new light on the structure of the nucleon. Among the most surprising results was the realization that only a small fraction of the nucleon spin (20% – 30%) is carried by the quark helicities, in disagreement with quark model expectations of 60% – 75%. This reduction is often attributed to the effect of a negatively polarized quark sea at low momentum fraction x , which is typically not included in quark models (see the paper by Isgur [14] for a detailed discussion).

For a more complete understanding of the quark structure of the nucleon, it is advantageous to concentrate on a kinematic region where the scattering is most likely to occur from a valence quark in the nucleon carry-

ing more than a fraction $x = 1/3$ of the nucleon momentum. In particular, the virtual photon asymmetry, $A_1(x) \approx g_1(x)/F_1(x)$, (where F_1 is the usual unpolarized structure function) can be (approximately) interpreted in terms of the polarization $\Delta u/u$ and $\Delta d/d$ of the valence u and d quarks in the proton in this kinematic region, while the contribution from sea quarks is minimized. This asymmetry also has the advantage of showing smaller scaling violations than the structure functions g_1 and F_1 individually [6, 8], making a comparison with various theoretical models and predictions more straightforward.

By measuring $A_1(x)$ at large x , one can test different predictions about the limit of $A_1(x)$ as $x \rightarrow 1$. Non-relativistic Constituent Quark Models (CQM) based on SU(6) symmetry predict $A_1(x) = 5/9$ for the proton, $A_1(x) = 0$ for the neutron and $A_1(x) = 1/3$ for the deuteron (modified by a factor $(1 - 1.5w_D)$ for the D-state probability w_D in the deuteron wave function). Quark models that include some mechanism of SU(6) symme-

try breaking (*e.g.*, one-gluon exchange hyperfine interaction between quarks [14]) predict that $A_1(x) \rightarrow 1$ for all three targets as x tends to 1. This is because target remnants with total spin 1 are suppressed relative to those with spin 0. The same limit for $x \rightarrow 1$ is also predicted by pQCD [15], because hadron helicity conservation suppresses the contribution from quarks anti-aligned with the nucleon spin. In this case, $A_1(x)$ would be predicted to be more positive at moderately large $x < 1$ because both u and d quarks contribute with positive polarization [16]. Finally, a recent paper [17] connected the behavior of $A_1(x)$ at large x with the dynamics of resonance production via duality, leading to several predictions for the approach to $A_1(x \rightarrow 1) = 1$ that depend on the mechanism of SU(6) symmetry breaking.

Clearly, measurements of the asymmetry A_1 at moderate to high $x \geq 0.3$ are an indispensable tool to improve our understanding of the valence structure of the nucleon. Although many data already exist on $A_1(x, Q^2)$, most of the high-energy data have very limited statistics at large x and therefore large uncertainties; high-precision data so far exist only for a ${}^3\text{He}$ target [11] (which can be used to approximate A_1 for a free neutron). Those data show for the first time a positive asymmetry A_1^n at large x , but agree better with predictions [14] that assume negative d -quark polarization $\Delta d/d$ even at large x .

In this paper, we report the first high-precision measurement of $A_1(x, Q^2)$ for the proton and the deuteron at moderate to large x ($x \geq 0.15$) over a range of momentum transfers $Q^2 = 0.05 \dots 5.0$ (GeV/c) 2 , covering both the resonance and the deep inelastic region.

The data described in this paper were collected during the second polarized target run (2000-2001) with CLAS in Hall B of the Thomas Jefferson National Accelerator Facility (TJNAF – Jefferson Lab). Results from the first run with beam energies of 4.2 and 2.5 GeV were recently published [12, 13]. The present data extend the kinematic coverage significantly to both lower and higher values of Q^2 (covering nearly two orders of magnitude, instead of only one), and to higher values of W , covering much more of the DIS region (nearly doubling the range in x). Longitudinally polarized electrons of several beam energies around 1.6 GeV and 5.7 GeV were scattered off longitudinally polarized ammonia targets — ${}^{15}\text{NH}_3$ and ${}^{15}\text{ND}_3$ — and detected in the CEBAF Large Acceptance Spectrometer (CLAS). A detailed description of CLAS may be found in Ref. [18]. The spectrometer is equipped with a superconducting toroidal magnet and three drift chamber regions that cover up to 80% of the azimuthal angles and reconstruct the momentum of charged particles scattering within a polar angular range between 8° and 142° . (Due to obstruction by the polarized target Helmholtz coils only scattering angles up to 50° were accessible during our experiment.) We used both the inbending (for electrons) and the outbending torus magnetic field orientations, to extend the coverage in Q^2 .

An array of scintillator counters covers the above angular range and is used to determine the time of flight for charged particles. A forward angle electromagnetic calorimeter 16 radiation lengths thick covers polar angles up to 45° and is used along with the drift chambers to separate pions from electrons for this analysis. A gas Cherenkov detector covering the same angular range as the calorimeter is used in conjunction with the calorimeter to create a coincidence trigger, and to reject pions.

The target material was kept in a 1 K liquid Helium bath and was polarized via Dynamic Nuclear Polarization (DNP) [19]. The target polarization was monitored online using a Nuclear Magnetic Resonance (NMR) system. The beam polarization was measured at regular intervals with a Møller polarimeter. The product of beam and target polarization ($P_b P_t$) was determined from the well-known asymmetry for elastic (quasielastic) scattering from polarized protons (deuterons), measured simultaneously with inelastic scattering. For the 1.6 GeV data set, the average polarization product was $P_b P_t = 0.54 \pm 0.005$ (0.18 ± 0.007) for the ${}^{15}\text{NH}_3$ (${}^{15}\text{ND}_3$) target. The corresponding values for the 5.7 GeV data set are 0.51 ± 0.01 and 0.19 ± 0.03 .

The data analysis proceeds along the following steps (see Ref. [13] for details). We first extract the raw count rate asymmetry $A_{||}^{raw} = (N^+ - N^-)/(N^+ + N^-)$, where the electron count rates for anti-parallel (N^+) and parallel (N^-) electron and target polarization are normalized to the (live-time gated) beam charge for each helicity. The background due to misidentified pions and electrons from decays into e^+e^- pairs has been subtracted from these rates. We divide the result by the product of beam and target polarization $P_b P_t$ and correct for the contribution from non-hydrogen nuclei in the target. For this purpose, we use auxiliary measurements on ${}^{12}\text{C}$, ${}^4\text{He}$ and pure ${}^{15}\text{N}$ targets. We then combine the asymmetries for different beam and target polarization directions, thereby reducing any systematic errors from false asymmetries (no significant differences between the different polarization sets were found). Finally we apply radiative corrections using the code RCSLACPOL [6] which follows the prescription by Kuchto and Shumeiko [20] for the internal corrections and by Tsai [21] for the external corrections. The (quasi-)elastic radiative tail contribution to the denominator of the asymmetry is treated as a further dilution factor f_{RC} .

The final result is the longitudinal (Born) asymmetry $A_{||} = D(A_1 + \eta A_2)$, where the depolarization factor $D = (1 - E'\epsilon/E)/(1 + \epsilon R)$, E (E') is the beam (scattered electron) energy, $\epsilon = (2EE' - Q^2/2)/(E^2 + E'^2 + Q^2/2)$ is the virtual photon polarization, $R \lesssim 0.2$ is the ratio of the longitudinal to the transverse photoabsorption cross section and $\eta = (\epsilon\sqrt{Q^2})/(E - E'\epsilon)$. A_2 is the longitudinal-transverse interference virtual photon asymmetry. We use the standard notations for the en-

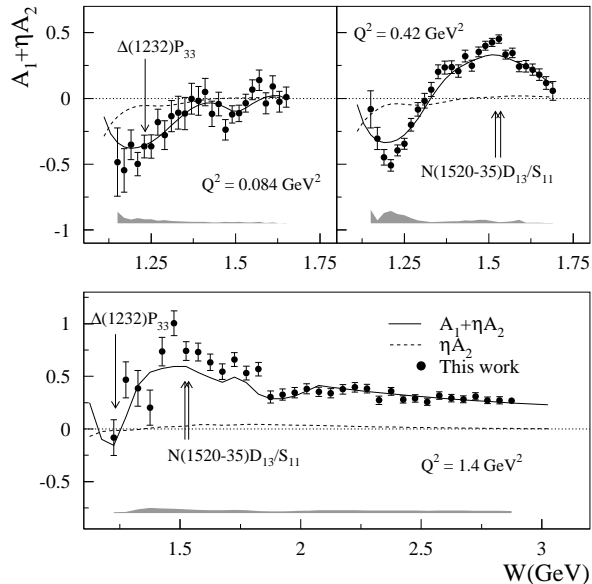


FIG. 1: Results for the asymmetry $A_{||}/D = A_1 + \eta A_2$ on the proton versus final-state invariant mass W , for three bins in Q^2 . Arrows indicate the masses of several resonances. The first two panels show data obtained with 1.6 GeV beam energy, while the last panel comes from the 5.7 GeV data. The solid line close to the data points is the result for $A_{||}/D$ of our parametrization of previous world data. The dashed line close to zero is the estimated contribution from the unmeasured asymmetry A_2 to $A_{||}/D$. Bands at the bottom of all figures indicate systematic errors.

ergy transfer, $\nu = E - E'$, and four-momentum transfer squared, $Q^2 = 4EE' \sin^2(\theta/2)$.

Finally, using a parametrization of the world data [6, 8] to model A_2 and R , we extract A_1 and the closely related ratio g_1/F_1 :

$$\frac{g_1}{F_1}(x, Q^2) = \frac{1}{(\gamma^2 + 1)} \left(\frac{A_{||}}{D} + (\gamma - \eta) A_2 \right) \quad (1)$$

with $\gamma^2 = Q^2/\nu^2$. The extraction of this ratio is typically less dependent on the unmeasured asymmetry, A_2 , than that of the asymmetry A_1 . Our parametrization includes input from phenomenological models AO [23] and MAID [24] as well as fits to the polarized data from the first run with CLAS [12, 13] and to unpolarized structure functions measured in Jefferson Lab's Hall C [22]. More details of the parametrization and the data analysis can be found in Ref. [13]. Since A_1 and g_1/F_1 are independent of beam energy for given (x, Q^2) values, we combine (after consistency checks) our results for each bin in (x, Q^2) for all beam energies and CLAS torus magnetic field settings.

To estimate systematic uncertainties on our final results, we vary all input parameters and models within realistic limits and study the induced variations of

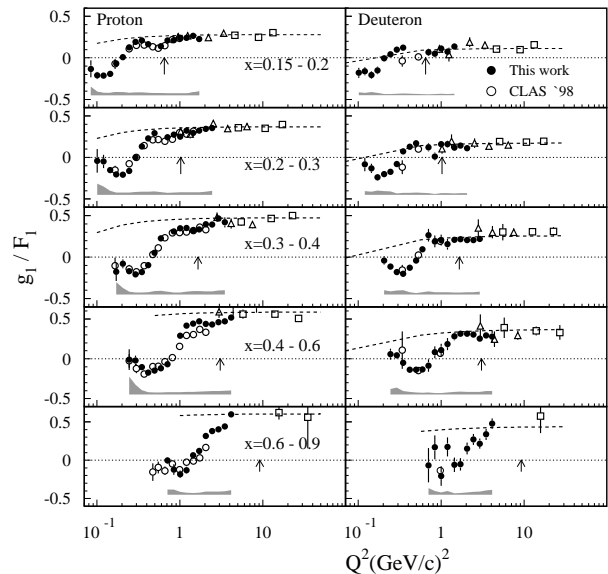


FIG. 2: Measured ratio g_1/F_1 as a function of momentum transfer squared Q^2 for several bins in x for the proton (left) and the deuteron (right). A few data points from SLAC experiments E143 [6] (open triangles) and E155 [8] (open squares) are also shown for comparison, as well as data from the first run with CLAS [12, 13] (open circles). The dashed line represents our parametrization of the world data in the DIS region [8]. Arrows indicate the conventional limit of the resonance region at $W = 2$ GeV.

the asymmetry A_1 . We then add all these variations in quadrature to get the total systematic uncertainty. Among the sources of systematic errors we considered are uncertainties on the product of beam and target polarization and various inputs in our determination of the dilution factor (target dimensions, nuclear cross sections, and contributions from polarized nuclei other than the hydrogen isotope under consideration). We also estimate the remaining contribution from misidentified pions and electrons from pair-symmetric decay processes. Finally, we varied all model parametrizations for unpolarized (F_1, R) and polarized (A_1, A_2) structure functions used both in the extraction of A_1 and g_1/F_1 and in our radiative corrections. Systematic errors are indicated by shaded bands in the figures.

A small sample of our results on the asymmetry $A_{||}/D$ for the proton is shown in Fig. 1. Since the asymmetry A_2 contributes only very little to these data (see dashed line in the figure), they are essentially equal to A_1 . A strong dependence of this asymmetry on the final state mass W can be seen, especially at low Q^2 (top left panel). Our total data set covers 19 bins in Q^2 , with similar statistics for the deuteron. The entire data set is available at the CLAS Physics Database (<http://clasweb.jlab.org/physicsdb/intro.html>). These data can be used to constrain transition amplitudes for resonances of different spin and isospin which par-

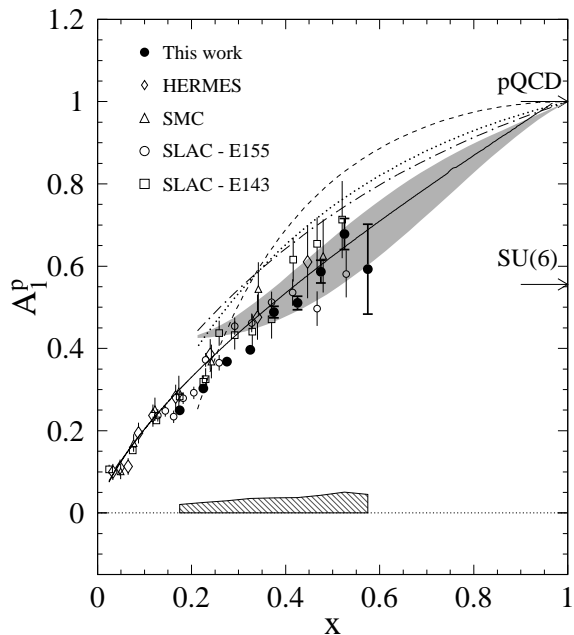


FIG. 3: Results for the asymmetry $A_1(x)$ on the proton. Filled circles show our data in the deep inelastic region ($W > 2$ GeV, $Q^2 > 1$ GeV²) while the remaining open symbols are for data from several previous experiments [4, 6, 8, 9]. The SU(6) expectation for all x is indicated by the arrow. The solid line shows our parametrization of the world data at a fixed $Q^2 = 10$ GeV². The shaded band covers a range of calculations by Isgur [14] that model the hyperfine-interaction breaking of SU(6) symmetry. The remaining three curves correspond to different scenarios of SU(6) symmetry breaking as presented in the paper by Close and Melnitchouk [17]: helicity-1/2 dominance (dashed), spin-1/2 dominance (dotted) and symmetric wave function suppression (dash-dotted).

tially overlap with each other and the non-resonant background. For instance, in the region of the $\Delta(1232)$, the asymmetry is negative at low Q^2 , since the transition to the Δ is dominated by the $A_{3/2}$ amplitude, while at larger Q^2 this amplitude seems to be suppressed and the non-resonant background becomes more dominant. Similarly, around $W = 1.53$ GeV, the asymmetry makes a rapid transition from being slightly negative at small Q^2 to large positive values even at rather moderate Q^2 , indicating that the $A_{3/2}$ amplitude for the transition to the D_{13} resonance becomes less important than the $A_{1/2}$ amplitude for the transition to both the D_{13} and S_{11} resonances.

The closely related ratio of structure functions, g_1/F_1 , is shown in Fig. 2 as a function of Q^2 , averaged over several bins in x . The new data are in good agreement with the results of the first run with CLAS [12, 13]. In the DIS region, both g_1 and F_1 are expected to have only logarithmic scaling violations, and their ratio has been found to be nearly independent of Q^2 in previous experiments (see, for example, the SLAC data [6, 8] reproduced

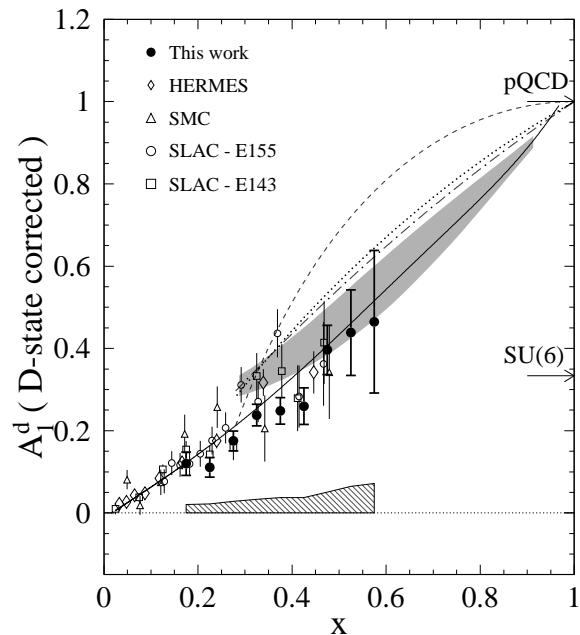


FIG. 4: Results for the asymmetry $A_1(x)$ on the deuteron. The lines and symbols have the same meaning as in Fig. 3. The data are divided by $(1 - 3/2w_D) \approx 0.925$ to correct for the deuteron D-state probability w_D , while the model predictions are for an isoscalar (proton plus neutron) target.

in Fig. 2). Our data show a clear decrease in this asymmetry with decreasing Q^2 ; in particular, for the proton they fall below the DIS parametrization around $Q^2 = 1$ GeV² and small x . This Q^2 -dependence becomes much more pronounced in the region of the nucleon resonances (at Q^2 below the limits indicated by arrows in Fig. 2), leading to a strong deviation of the data from a smooth extrapolation of DIS data [8] (dashed lines in Fig. 2). This is a direct consequence of the fact that W varies with Q^2 at fixed x and reflects the W -dependence seen in Fig. 1. For kinematics corresponding to the excitation of the Δ resonance (at the lowest Q^2 in each panel), the asymmetry is much reduced and even changes sign relative to the DIS region at small Q^2 due to the dominance of the $A_{3/2}$ amplitude. The data above $W = 2$ GeV can be incorporated into NLO fits of spin structure functions to improve the precision with which polarized parton distribution functions are known.

The results for $A_1(x)$, averaged over $Q^2 > 1$ GeV² and $W > 2$ GeV, are shown in Fig. 3 for the proton and in Fig. 4 for the deuteron. At small x , where our average Q^2 is close to 1 GeV², the data fall below our parametrization of the world data with $Q^2 = 10$ GeV² (solid line). This deviation is due to the Q^2 -dependence shown in Fig. 2 (note that A_1 and g_1/F_1 are very close in this kinematic region). In contrast, both of our data sets exceed the SU(6) limits at x above 0.45. The hyperfine interaction model of SU(6) symmetry breaking by

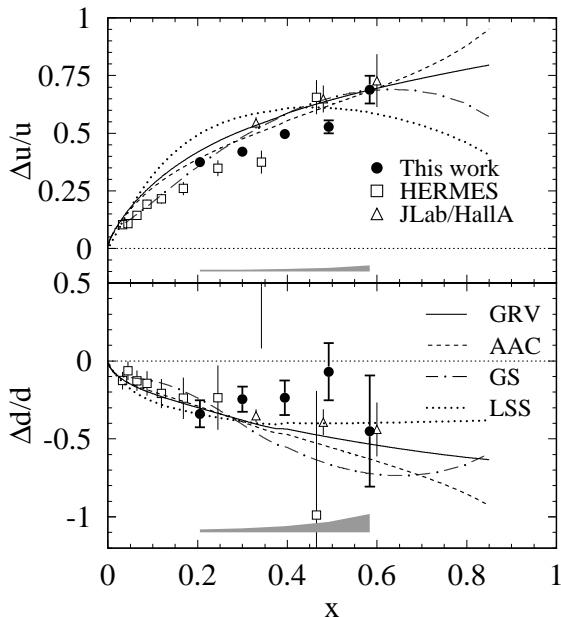


FIG. 5: Quark polarizations $\Delta u/u$ and $\Delta d/d$ extracted from our data. Included are all data above $W = 1.77$ GeV and $Q^2 = 1$ GeV². Also shown are semi-inclusive results from Hermes [9] and inclusive results from Hall A data [11] combined with previous data from CLAS [12]. The solid line is from the NLO fit to the world data by GRV [25], the dashed line is from the AAC fit [26], the dash-dotted line is from Gehrmann and Stirling [27] and the dotted line indicates the latest fit from LSS [28].

Isgur [14] (grey band in figures) is closest to the data. Of the different mechanisms for SU(6) symmetry breaking considered by Close and Melnitchouk [17], the model with suppression of the symmetric quark wave function (dot-dashed curve in Figs. 3,4) deviates least from the data. In general, our results are in better agreement with models (like the two mentioned above) in which the ratio of down to up quarks, d/u , goes to zero and the polarization of down quarks, $\Delta d/d$ tends to stay negative for rather large values of x , in contrast to the behavior expected from hadron helicity conservation [15, 16]. This is also in agreement with the findings by the experiment on ³He [11] in Jefferson Lab's Hall A.

Within a naive quark-parton model (and ignoring any contribution from strange quarks), we can estimate the quark polarizations $\Delta u/u$ and $\Delta d/d$ directly from our data by combining the results for g_1 from the proton and the deuteron (including some nuclear corrections for the deuteron D-state and Fermi motion) with our parametrization of the world data on F_1^p and F_1^D :

$$\frac{\Delta u}{u} \approx \frac{5g_{1p} - 2g_{1d}/(1 - 1.5w_D)}{5F_{1p} - 2F_{1d}}; \quad (2)$$

$$\frac{\Delta d}{d} \approx \frac{8g_{1d}/(1 - 1.5w_D) - 5g_{1p}}{8F_{1d} - 5F_{1p}}. \quad (3)$$

The result (Fig. 5) has relatively large statistical errors for $\Delta d/d$, since neither A_1^p nor A_1^d are very sensitive to $\Delta d/d$. (We included data down to $W = 1.77$ GeV in our estimate for the highest x points to reduce those errors somewhat; at these rather large values of $Q^2 > 3$ (GeV/c)² we expect little deviation from the DIS limit in this W range). Our estimate is consistent with the result from the ³He experiment [11], showing no indication of a sign change to positive values up to $x \approx 0.6$. At the same time, our data for $\Delta u/u$ are the statistically most precise available at this time, and show a consistent trend towards $\Delta u/u = 1$ at our highest x points. While the absolute values of $\Delta u/u$ and $\Delta d/d$ might be somewhat different from more sophisticated NLO DGLAP analyses (like the curves shown in Fig. 5), the error bars in Fig. 5 give an indication of the possible improvement in precision when our data are included in such fits.

In summary, we have measured the virtual photon asymmetry A_1 and the related ratio g_1/F_1 of structure functions on the proton and the deuteron with unprecedented precision, at high x and over a large kinematic range in x and Q^2 . Our data span the resonance region $W < 2$ GeV and extend into the DIS region. They contribute to our knowledge of the valence quark structure of the nucleon and its excited states, and can be used to improve NLO fits for the extraction of polarized parton distribution functions. Our data confirm a clear increase in the polarization of valence u quarks at high x as expected by pQCD and various models of SU(6) symmetry breaking; on the other hand, the polarization of the d quarks seems to remain negative up to the highest values of x accessible to our experiment. Future measurements, in particular with the energy-upgraded Jefferson Lab accelerator, will be able to extend these data with improved precision to higher values of x (exceeding $x \approx 0.8$), allowing a definite test of various models of SU(6) symmetry breaking.

Acknowledgments

We would like to acknowledge the outstanding efforts of the staff of the Accelerator and the Physics Divisions at Jefferson Lab that made this experiment possible. This work was supported in part by the Italian Istituto Nazionale di Fisica Nucleare, the French Centre National de la Recherche Scientifique, the French Commissariat à l'Énergie Atomique, the U.S. Department of Energy and National Science Foundation, the Emmy Noether grant from the Deutsche Forschungsgemeinschaft and the Korean Science and Engineering Foundation. The Southeastern Universities Research Association (SURA) operates the Thomas Jefferson National Accelerator Fa-

cility for the United States Department of Energy under contract DE-AC05-84ER-40150.

-
- * Current address: Thomas Jefferson National Accelerator Facility, Newport News, Virginia 23606
† Electronic address: skuhn@odu.edu; Corresponding author.
‡ Current address: Massachusetts Institute of Technology, Cambridge, Massachusetts 02139-4307
§ Current address: Ohio University, Athens, Ohio 45701
¶ Deceased
** Current address: University of New Hampshire, Durham, New Hampshire 03824-3568
†† Current address: Moscow State University, General Nuclear Physics Institute, 119899 Moscow, Russia
‡‡ Current address: Los Alamos National Laboratory, Los Alamos, New Mexico 87545
§§ Current address: Catholic University of America, Washington, D.C. 20064
¶¶ Current address: Physikalisches Institut der Universität Giessen, 35392 Giessen, Germany
*** Current address: University of Massachusetts, Amherst, Massachusetts 01003
- [1] M. J. Alguard et al., Phys. Rev. Lett. **41**, 70 (1978).
[2] G. Baum et al., Phys. Rev. Lett. **51**, 1135 (1983).
[3] J. Ashman et al. (EMC), Nucl. Phys. **B328**, 1 (1989).
[4] B. Adeva et al. (SMC), Phys. Rev. D **58**, 112001 (1998).
[5] P. L. Anthony et al. (E142), Phys. Rev. D **54**, 6620 (1996), hep-ex/9610007.
[6] K. Abe et al. (E143), Phys. Rev. D **58**, 112003 (1998), hep-ph/9802357.
[7] K. Abe et al. (E154), Phys. Rev. Lett. **79**, 26 (1997), hep-ex/9705012.
[8] P. L. Anthony et al. (E155), Phys. Lett. **B493**, 19 (2000), hep-ph/0007248.
[9] A. Airapetian et al. (HERMES), Phys. Rev. D **71**, 012003 (2005), hep-ex/0407032.
[10] M. Amarian et al. (Jefferson Lab E94-010), Phys. Rev. Lett. **92**, 022301 (2004), hep-ex/0310003.
[11] X. Zheng et al. (Jefferson Lab Hall A), Phys. Rev. C **70**, 065207 (2004), nucl-ex/0405006.
[12] R. Fatemi et al. (CLAS), Phys. Rev. Lett. **91**, 222002 (2003), nucl-ex/0306019.
[13] J. Yun et al. (CLAS), Phys. Rev. C **67**, 055204 (2003), hep-ex/0212044.
[14] N. Isgur, Phys. Rev. D **59**, 034013 (1999), hep-ph/9809255.
[15] G. R. Farrar and D. R. Jackson, Phys. Rev. Lett. **35**, 1416 (1975).
[16] S. J. Brodsky, M. Burkardt and I. Schmidt, Nucl. Phys. **B441**, 197 (1995).
[17] F. E. Close and W. Melnitchouk, Phys. Rev. C **68**, 035210 (2003), hep-ph/0302013.
[18] B. A. Mecking et al. (CLAS), Nucl. Inst. Meth. **A503**, 513 (2003).
[19] C. D. Keith et al., Nucl. Inst. Meth. **A501**, 327 (2003).
[20] T. V. Kukhto and N. M. Shumeiko, Nucl. Phys. **B219**, 412 (1983).
[21] Y.-S. Tsai, Rev. Mod. Phys. **46**, 815 (1974).
[22] M. E. Christy, private communication, (2005).
[23] V. Burkert and Z. Li, Phys. Rev. D **47**, 46 (1993).
[24] D. Drechsel and L. Tiator, J. Phys. G **18**, 449 (1992).
[25] M. Glück, E. Reya, M. Stratmann, and W. Vogelsang, Phys. Rev. D **63**, 094005 (2001).
[26] Y. Goto et al. (Asymmetry Analysis collaboration), Phys. Rev. D **62**, 034017 (2000).
[27] T. Gehrman and W. J. Stirling, Phys. Rev. D **53**, 6100 (1996), hep-ph/9512406.
[28] E. Leader, A. V. Sidorov and D. B. Stamenov, Phys. Rev. D **73**, 034023 (2006).